Available online at www.sciencedirect.com
ScienceDirect
Tetrahedron 64 (2008) 2027–2034
Tetrahedron
www.elsevier.com/locate/tet

Chloraholides C–F: a new class of potent and selective potassium channel blockers from *Chloranthus holostegius*

Sheng-Ping Yang, Zhao-Bing Gao, Yan Wu, Guo-Yuan Hu, Jian-Min Yue*

State Key Laboratory of Drug Research, Shanghai Institute of Materia Medica, Shanghai Institutes for Biological Sciences, Chinese Academy of Sciences, 555 Zu Chong Zhi Road, Zhangjiang Hi-Tech Park, Shanghai 201203, PR China

Received 15 October 2007; received in revised form 19 December 2007; accepted 21 December 2007
Available online 4 January 2008

Abstract

Four unusually fused polycyclic sesquiterpenoid dimers, chloraholides C–F (**1**–**4**), were isolated from the whole plant of *Chloranthus holostegius*. Their structures and absolute configurations were established by spectroscopic methods, including 2D NMR and CD spectra. Chloraholides C–F (**1**–**4**) exerted potent and selective inhibition on the delayed rectifier (I_K) K^+ current with the IC_{50} values of 3.6±10.1, 2.7±0.3, 27.5±5.1 and 57.5±6.1 μM, respectively.

Keywords: Chloraholides C–F; Potassium channel blocker; Structural elucidation; *Chloranthus holostegius*

1. Introduction

Potassium (K^+) channels that regulate a variety of physiological processes in both electrically excitable and non-excitable cells have been implicated in the pathogenesis of severe human diseases such as long-QT syndromes, episodic ataxia/myokymia, familial convulsions, hearing and vestibular diseases, Bartter's syndrome and familial persistent hyperinsulinemic hypoglycemia of infancy.[1] In addition, changes in K^+ channel function have been associated with cardiac hypertrophy and failure, apoptosis and oncogenesis and various neurodegenerative and neuromuscular disorders.[1–3] The advances in K^+ channel studies have facilitated the exploitations of potassium (K^+) channels as therapeutic targets by pharmacological approaches, and a great number of organic modulators of potassium (K^+) channels have been developed into new drugs or drug candidates.[1,4]

The plants belonging to the genus of *Chloranthus* (Chloranthaceae) mainly grow in the east of Asia.[5] There are ca. 13 species and 5 variations occurring in China,[6] and most of them have applications in folk medicine to treat bone fracture.[7] Phytochemical investigations on this plant genus have led to the isolation of a number of sesquiterpenoids[8] and sesquiterpenoid oligomers.[9] Most secondary metabolites of *Chloranthus* genus isolated hitherto are sesquiterpenoids and sesquiterpenoid dimers.[9] Recently, the dimeric sesquiterpenoids, shizukaol B, cycloshizykaol A and shizukaol F obtained from *chloranthus japonicus* have been reported to inhibit the expression of cell adhesion molecules.[10] A previous study on *Chloranthus holostegius* (Hand.-Mazz.) Pei et Shan reported the isolation of several sterols, coumarins and one lindenane sesquiterpenoid.[11] In our recent study, two dimeric sesquiterpenoids, chloraholides A and B with potent inhibition on the delayed rectifier (I_K) K^+ current were isolated from the whole plant of *C. holostegius*.[9d] As the continuation of this work, four additional novel sesquiterpenoid dimers (Fig. 1), chloraholides C–F (**1**–**4**) were further identified from the same plant material. Chloraholides C–F (**1**–**4**) exhibited potent and selective potassium channel blocking activity on the delayed rectifier (I_K) K^+ current with the IC_{50} values of 3.6±10.1, 2.7±0.3, 27.5±5.1 and 57.5±6.1 μM, respectively. It is noteworthy that chloraholide D (**2**) is 388-fold more

* Corresponding author. Tel./fax: +86 21 50806718.
E-mail address: jmyue@mail.shcnc.ac.cn (J.-M. Yue).

0040-4020/$ - see front matter © 2008 Elsevier Ltd. All rights reserved.
doi:10.1016/j.tet.2007.12.057

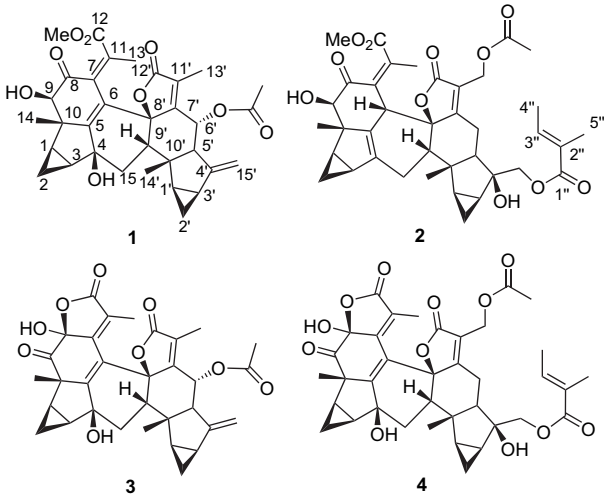

Figure 1. Structures of chlorahololides C–F (**1**–**4**).

potent than tetraethylammonium chloride, a classical blocker of the delayed rectifier K^+ current with an IC_{50} value of 1.05± 0.21 mM. Herein, we report the isolation and the in-depth structural characterization of chlorahololides C–F (**1**–**4**), along with their potent and selective potassium channel blocking activities.

2. Results and discussion

2.1. Structural elucidation

Chlorahololide C (**1**) was obtained as a tiny prismatic crystal (from CH_3OH) with optical rotation $[\alpha]_D^{20}$ −143. The molecular formula of **1**, as determined by HREIMS at *m/z* 576.2359 $[M]^+$, is $C_{33}H_{36}O_9$ with 16 double bond equivalents. The positive mode ESI MS ion at 599 $[M+Na]^+$ further secured its molecular formula. The IR absorptions revealed the presence of carbonyl (1755 and 1709 cm^{-1}) and hydroxyl (3479 cm^{-1}) functionalities. In the ^1H NMR spectrum (Table 1), two broad singlets at δ 3.48 and 2.62 (each ca. 1H), which did not show any correlations in the HSQC spectrum, were indicative of exchangeable protons, such as hydroxyls. In accord with the molecular formula, 33 carbon signals were resolved in the ^{13}C NMR spectrum (Table 2), and categorized by DEPT experiments as four carbonyls (δ_C 199.5, 172.8, 171.0 and 170.2), six methyls, three persubstituted double bonds, one exocyclic double bond, three sp^3 methylenes, eight sp^3 methines and four sp^3 quaternary carbons. Of the six methyls, two were readily attributable to a methoxyl (δ_C 52.4, δ_H 3.76) and an acetoxyl (δ_C 20.6, δ_H 2.04), the latter was confirmed by HMBC correlation (Fig. 2). On the biogenetic reasoning and the fact of occurrence of dimeric sesquiterpenoids within this plant genus, the remaining 30 carbons comprising its scaffold suggested that compound **1** was a sesquiterpenoid dimer. The functionalities distinguished above accounted for eight degrees of unsaturation, and an octacyclic core was thus required for **1** to consume the remaining eight double bond equivalents.

The scaffold of **1** was constructed by a comprehensive collation of the 2D NMR data including ^1H–^1H COSY, HSQC, and HMBC spectra. The ^1H, ^{13}C NMR and HSQC spectra allowed all protons to be attributed to their respective bonding carbons. Four proton bearing and spin coupling subunits as drawn with bold bonds (Fig. 2) were established by ^1H–^1H COSY spectrum. The connectivity of four structural subunits and most other functional groups was achieved via the observed ^2J and ^3J HMBC correlations (Fig. 2), leaving only the linkages of C-6/C-7 and C-8′/C-12′ in the polycyclic core of **1** unsettled. Fortunately, an apparent ^4J HMBC correlation between H_3-13 and C-6 was served to link the C-6 and C-7 bond. The chemical shift of C-8′ at δ 86.3 implied a linkage between the C-8′ and C-12′ via an oxygen atom to form an α,β-unsaturated γ-lactone, as in the cases of chloramultilide A[9c] and chlorahololide A.[9d] The methoxyl and acetoxyl groups were attached to C-12 and C-6′, respectively, based on the HMBC correlations of OMe/C-12 and H-6′/carbonyl of Ac. The oxygenated quaternary carbon at δ 78.2 was attributed to C-4 bearing a hydroxyl, as judged by the HMBC correlations of H-1, H_2-2 and H_2-15 to C-4. The spectral analysis described above well defined the plane structure of chlorahololide C (**1**) being a lindenane sesquiterpenoid dimer.

The relative configuration of **1** was established by a performance of ROESY experiment (Fig. 3), in which, the correlations of H-1/H-3, H-1/H-2α, H-3/H-2α, H-1′/H-3′, H-1′/H-2′α, H-3′/H-2′α, H-5′/H-9 and H-5′/H-15α indicated that they were co-facial and were arbitrarily fixed to be α-orientated. In consequence, the ROESY cross-peaks of H-2β/H_3-14, H_3-14′/H-2′β and H-6′/H_3-14′ revealed that CH_3-14, CH_3-14′ and H-6′ were β-configuration. The 4-OH at δ 2.62 (each ca. 1H) showed ROESY correlations to H_2-2, H-9′ and H-15β indicated that was β-directed, which is consistent with that of chlorahololide A, whose relative configuration was determined by X-ray crystallography.[9d] A biogenetic hypothesis (Scheme 1) based on an enzymatic Diels–Alder cycloaddition[12] of two molecular lindenane sesquiterpenoids (components A and B) was proposed for chlorahololide C (**1**) that inherited the anticipated stereochemistry by following the *cis* and *endo* rule of Diels–Alder cycloaddition.[13] A key ROESY correlation between H-9 and H-5′ verified that **1** was a typical *endo*-cycloaddition product of two lindenane sesquiterpenoids. Accordingly, the C-8′–O bond and H-9′ were theoretically co-facial and β-orientated, and was substantiated by the ROESY correlation of CH_3-14′β/H-9′. Finally, the strong ROESY correlation between H_3-13 and H_3-13′ indicated that they were co-facial, suggesting that the $\Delta^{7(11)}$ double bond took 7*Z*-geometry.

Chlorahololide D (**2**) showed a molecular formula $C_{38}H_{44}O_{11}$ as determined by HREIMS at *m/z* 676.2850 $[M]^+$ (calcd 676.2884). Its ^1H and ^{13}C NMR data (Tables 1 and 2) revealed functionalities of methoxyl, an acetoxyl and a 2-methylbut-2-enoxyl groups. The olefinic proton signal at δ_H 6.90 indicated that the 2-methylbut-2-enoxyl with *E*-geometry (for the *E*-geometry, the olefinic proton signal normally appears at ca. δ 6.60–7.15 in the ^1H NMR, while for the *Z*-geometry, it is around δ 6.06)[14] was tigloyloxyl. Excluding the aforementioned substituents, the central skeleton of lindenane sesquiterpenoid dimer was implied by the ^1H and ^{13}C NMR spectra, which showed great similarity to those of **1**, suggesting that **2** was an analogue of this compound class. Comprehensive

Table 1
^{1}H NMR data of chlorahololides C–F (**1**–**4**)

	1[a]	**2**[a]	**2**[b]	**3**[a]
1	2.03 (m)	2.05 (m)	2.32 (m)	2.33 (ddd, 8.6, 6.8, 4.2)
2α	0.96 (m, 2H)	1.00 (m)	0.97 (ddd, 7.8, 7.4, 4.2)	1.04 (ddd, 8.6, 8.6, 6.2)
2β		0.30 (ddd, 4.4, 4.2, 2.9)	0.38 (m)	1.27 (m)
3	1.90 (m)	1.83 (m)	1.95 (m)	1.84 (ddd, 10.5, 6.8, 4.0)
6		3.92 (d, 3.6)	4.20 (d, 3.0)	
9	3.84 (d, 2.7)	3.95 (s)	4.39 (s)	
13	1.63 (s, 3H)	1.88 (d, 0.3, 3H)	2.11 (s, 3H)	1.61 (s, 3H)
14	1.08 (s, 3H)	1.02 (s, 3H)	1.34 (s, 3H)	1.18 (s, 3H)
15α	1.86 (m)	2.77 (dd, 16.4, 1.3)	2.83 (br d, 17.7)	1.96 (dd, 16.3, 14.0)
15β	2.81 (dd, 13.6, 6.7)	2.59 (ddd, 16.4, 5.9, 4.1)	2.64 (ddd, 16.3, 5.5, 4.4)	2.77 (dd, 16.3, 6.7)
1′	1.62 (m)	1.56 (ddd, 8.7, 7.8, 4.1)	1.71 (m)	1.62 (m)
2′α	0.82 (ddd, 8.5, 8.5, 5.1)	0.72 (ddd, 8.9, 8.7, 5.7)	0.75 (ddd, 8.8, 8.5, 5.5)	0.85 (ddd, 8.6, 8.6, 5.4)
2′β	0.66 (ddd, 5.1, 3.5, 3.4)	1.27 (ddd, 5.7, 4.6, 4.1)	1.55 (m)	0.70 (ddd, 5.4, 3.8, 3.7)
3′	1.99 (m)	1.50 (m)	1.48 (ddd, 8.8, 8.1, 3.3)	2.02 (m)
5′	2.60 (m)	1.76 (dd, 13.7, 5.9)	2.12 (m)	3.01 (ddd, 11.0, 2.6, 2.5)
6′α		2.35 (dd, 18.6, 5.9)	2.89 (dd, 18.4, 5.8)	
6′β	5.61 (d, 10.8)	2.73 (dd, 18.6, 13.7)	3.24 (dd, 18.4, 13.7)	5.76 (d, 11.0)
9′	2.83 (dd, 14.0, 6.7)	1.86 (m)	1.95 (m)	2.78 (dd, 14.0, 6.7)
13′a	2.08 (s, 3H)	4.82 (d, 13.9)	5.15 (d, 12.7)	2.01 (s, 3H)
13′b		4.77 (d, 13.9)	5.10 (d, 12.7)	
14′	0.72 (s, 3H)	0.86 (s, 3H)	1.09 (s, 3H)	0.78 (s, 3H)
15′a	5.02 (d, 1.3)	4.21 (d, 11.7)	4.64 (d, 11.3)	5.04 (dd, 2.8, 1.3)
15′b	4.65 (s)	3.81 (d, 11.7)	4.14 (d, 11.3)	4.68 (dd, 2.7, 2.3)
3″		6.90 (m)	6.95 (m)	
4″		1.85 (d, 6.7, 3H)	1.65 (dd, 6.8, 0.9, 3H)	
5″		1.86 (s, 3H)	1.84 (s, 3H)	
O*Me*	3.76 (s, 3H)	3.76 (s, 3H)	3.65 (s, 3H)	
CO*Me*	2.04 (s, 3H)	2.08 (s, 3H)	2.07 (s, 3H)	1.98 (s, 3H)
OH	3.48 (br s)	NB	7.97 (br s)	2.52 (br s)
	2.62 (br s)	NB	6.38 (br s)	NB

	3[b]	**4**[a]	**4**[b]
1	2.31 (ddd, 8.6, 6.8, 4.5)	2.29 (m)	2.44 (m)
2α	0.95 (ddd, 8.6, 8.6, 5.8)	1.02 (m)	1.02 (ddd, 8.8, 8.7, 5.9)
2β	1.52 (ddd, 6.8, 4.2, 4.0)	1.21 (m)	1.47 (m)
3	1.96 (m)	1.81 (m)	2.07 (m)
13	1.85 (s, 3H)	1.70 (s, 3H)	1.94 (s, 3H)
14	1.17 (s, 3H)	1.17 (s, 3H)	1.15 (s, 3H)
15α	2.15 (dd, 13.2, 11.2)	1.78 (m)	2.26 (dd, 13.2, 10.9)
15β	2.98 (dd, 13.2, 6.5)	2.74 (dd, 13.8, 6.7)	3.07 (dd, 13.2, 6.8)
1′	1.61 (m)	1.57 (m)	1.81 (m)
2′α	0.69 (ddd, 8.4, 8.4, 5.0)	0.63 (ddd, 9.0, 8.6, 5.7)	0.66 (ddd, 9.0, 8.8, 4.6)
2′β	0.63 (ddd, 5.0, 3.9, 3.7)	1.21 (m)	1.47 (m)
3′	1.90 (m)	1.64 (m)	1.59 (m)
5′	3.75 (ddd, 10.9, 2.6, 2.4)	2.20 (dd, 12.8, 7.0)	2.99 (dd, 12.4, 7.4)[c]
6′α		2.36 (dd, 18.0, 7.0)	2.96 (dd, 15.2, 7.4)[c]
6′β	5.97 (d, 10.9)	2.95 (dd, 18.0, 12.8)	3.45 (m)[c]
9′	3.21 (dd, 11.2, 6.5)	2.66 (dd, 10.2, 6.7)	3.27 (dd, 10.9, 6.6)
13′a	2.10 (s, 3H)	4.87 (d, 12.7)	5.24 (d, 12.8)
13′b		4.82 (d, 12.7)	5.17 (d, 12.8)
14′	0.72 (s, 3H)	1.00 (s, 3H)	1.25 (s, 3H)
15′a	5.10 (br d, 2.0)	4.07 (d, 11.4)	4.72 (d, 10.9)
15′b	5.01 (br s)	4.05 (d, 11.4)	4.53 (d, 10.9)
3″		6.85 (m)	6.84 (m)
4″		1.81 (br d, 5.1, 3H)	1.53 (dd, 7.1, 0.8, 3H)
5″		1.80 (s, 3H)	1.74 (s, 3H)
CO*Me*	2.29 (s, 3H)	2.07 (s, 3H)	2.04 (s, 3H)
OH	11.7 (br s)	2.80 (br s)	12.2 (br s)
	6.76 (br s)	NB	6.96 (br s)
		NB	6.65 (br s)

'NB' not observed.
[a] Measured in $CDCl_3$.
[b] Measured in pyridine-d_5.
[c] Comprehensive ABX spin system.

Table 2
^{13}C NMR data ($CDCl_3$, 400 MHz) of chlorahololides C–F (**1**–**4**)

	1	2	3	4
1	26.0	25.7	24.5	24.2
2	8.7	15.9	9.6	9.3
3	30.1	24.7	30.2	30.1
4	78.2	142.3	76.8	77.0[a]
5	163.3	131.7	162.5	161.0
6	124.8	40.8	122.2	123.0
7	130.0	147.6	150.0	149.2
8	199.5	200.4	94.8	94.5
9	77.9	80.1	197.9	199.6
10	50.6	51.0	56.9	56.9
11	140.0	131.4	126.6	127.5
12	170.2	170.4	170.3	170.5
13	19.9	20.3	10.7	11.2
14	15.5	15.2	21.6	21.0
15	41.0	25.3	39.8	40.0
1′	25.4	25.2	24.9	26.6
2′	16.2	11.9	16.4	10.5
3′	23.9	28.2	24.1	29.6
4′	148.6	77.4	148.3	77.0[a]
5′	58.5	60.4	57.2	53.0
6′	64.0	22.6	64.8	22.6
7′	156.4	172.1	155.2	170.5
8′	86.3	93.2	84.8	85.4
9′	50.8	55.6	50.2	51.3
10′	41.7	44.6	42.1	44.5
11′	133.3	123.6	133.7	123.6
12′	172.8	171.3	171.5	170.5
13′	9.5	55.0	10.1	55.3
14′	23.1	26.3	23.4	24.2
15′	108.4	70.7	108.6	71.0
1″		168.2		168.5
2″		127.9		128.0
3″		138.8		139.0
4″		14.5		14.5
5″		12.1		12.1
O*Me*	52.4	52.5		
*CO*Me	171.0	170.3	168.9	170.4
CO*Me*	20.6	20.4	20.5	20.5

[a] Overlapped with $CDCl_3$.

analysis of 2D NMR data including $^1H-^1H$ COSY, HSQC, HMBC (Supplementary data S3) and ROESY (Fig. 4) led to the construction of the structure of **2**. In the HMBC, the correlations of H_2-15′/C-1″ and H-13′/acetoxyl allowed the linkages of the tigloyloxyl and the acetoxyl groups to C-15′ and C-13′, respectively. An oxygenated sp^3 quaternary carbon resonance at δ 77.4 was assigned to the C-4′ bearing a hydroxyl as judged

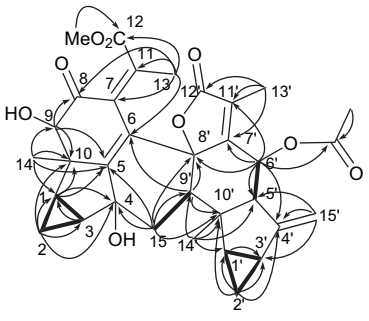

Figure 2. $^1H-^1H$ COSY (▬) and selected HMBC correlations (H→C) of chlorahololide C (**1**).

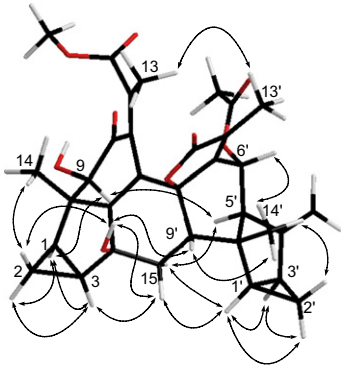

Figure 3. Key ROESY correlations (↔) of chlorahololide C (**1**).

from the HMBC correlations from H_2-15′, H-5′ and H-3′ to C-4′. The presence of a hydroxyl at C-9 (at δ 80.1) was also confirmed by the HMBC correlations of H_3-14/C-9, and H-9/C-5, C-8, and C-10. A Δ^4 double bond was revealed by the HMBC correlations of H_3-14/C-5, H-9/C-5, H-6/C-4, and H_2-15/C-4 and C-5. Comparison of the NMR data of **2** with those of **1** indicated that C-6 (at δ 40.8) of **2** was saturated to become a methine group, which was verified by the HMBC correlations from H-6 to C-4, C-7, C-8, C-11 and C-8′. The key ROESY cross-peak between H-6 and H-9′β showed that H-6 was β-configuration. Comparison of the ^1H NMR data of **2** as measured in different solvents of $CDCl_3$ and pyridine-d_5 (Table 1 and Fig. 4) showed significant pyridine-induced solvent shifts for H_3-14′ [$\Delta\delta=\delta$ ($CDCl_3$)$-\delta$ (pyridine-d_5)$=-0.23$] and H-2′β ($\Delta\delta$ -0.28), suggesting that 4′-OH was β-configuration,[15] and supported by the ROESY correlations of H_2-15′/H-5′ and H_2-15′/H-3′. The complete assignments of the ^1H and ^{13}C NMR of **2** were achieved by a combination of 2D NMR analysis.

Chlorahololide E (**3**) was found to have a molecular formula of $C_{32}H_{32}O_9$ on the basis of HREIMS at *m/z* 560.2071 $[M]^+$ (calcd 560.2046), with 17 degrees of unsaturation. The ^1H and ^{13}C NMR data of **3** resembled those of **1**, suggesting a close structural relationship. Compared with ^{13}C NMR data of compound **1**, the downfield shifted carbon signal at δ 150.0, and the upfield shifted carbon signal at δ 94.8 being attributable to C-7 and C-8 of **3**, respectively, and the absence of the methoxyl at C-12 (as indicated by both ^1H and ^{13}C NMR spectra) suggested that an α,β-unsaturated γ-lactone was formed via an ether linkage between C-8 and C-12, which also led to the formation of a hemi-ketal at C-8. This was confirmed by the HMBC correlation (^4J) between H_3-13 and C-8 (Supplementary data S4). A carbon signal at δ 197.9 was attributed to the C-9 ketone group by the strong HMBC correlation (^3J) between H_3-14 and C-9. The spectral data also revealed that the eastern hemisphere of **3** was identical with that of **1**. Although the ROESY spectrum could not provide the convincing information to assign stereochemistry of C-8, the significant pyridine-induced solvent shift [$\Delta\delta=\delta$ ($CDCl_3$)$-\delta$ (pyridine-d_5)$=-0.74$][15] of H-5′ (Table 1 and Supplementary data S4) clearly indicated that 8-OH possessed the α-configuration. The 2D NMR data (Supplementary data S4) fully supported the structural assignment of chlorahololide E (**3**).

Chlorahololide F (**4**) had a molecular formula of $C_{37}H_{40}O_{12}$ as determined by HREIMS at *m/z* 676.2508 $[M]^+$ (calcd 676.2520).

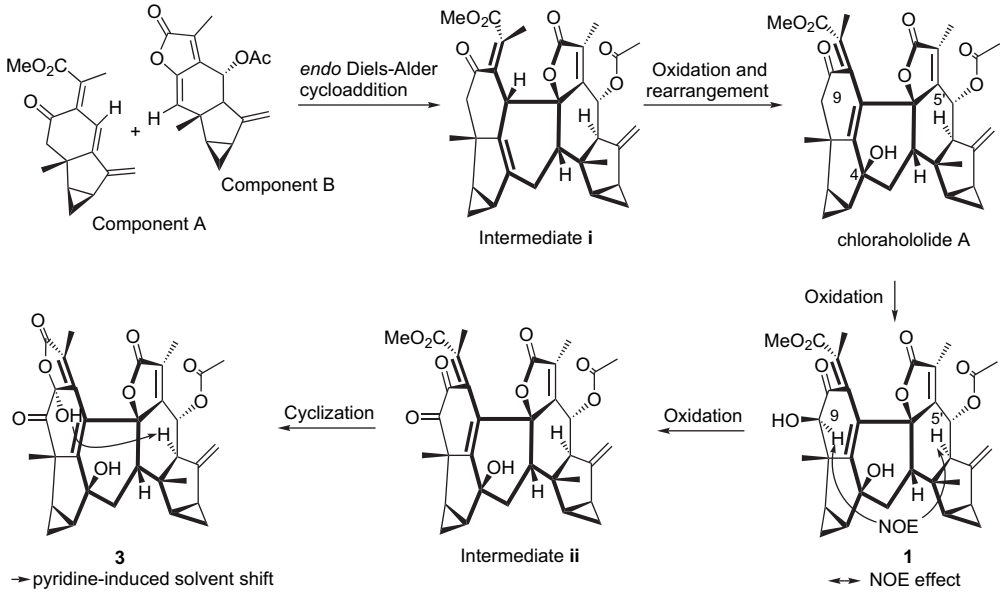

Scheme 1. Biogenetic pathway proposed for chlorahololides C (**1**) and E (**3**).

The ^{1}H and ^{13}C NMR data of **4** (Tables 1 and 2) closely resembled the spectral data of **3** except for the differences arising from the structural changes in the eastern hemisphere of the molecule. In comparison with **3**, the ^{1}H and ^{13}C NMR data of **4** indicated the presence of a C-6′ methylene, and the H_2-6′ resonated at δ_H 2.95 and 2.36 showing HMBC correlations to C-4′, C-5′, C-7′, C-8′ and C-11′ (Supplementary data S5). In the HMBC spectrum, an oxygenated quaternary carbon at δ_C 77.0 correlating with H-1′, H-3′ and H_2-6′ was assigned to C-4′ bearing a hydroxyl. The oxygenated carbon signals at δ_C 55.3 and 71.0 of two methylenes were assigned to C-13′ and C-15′ on the basis of HMBC correlations of H_2-13′/C-11′, C-12′ and C-7′, and H_2-15′/C-3′, C-4′ and C-5′, respectively. The NMR data of **4** also revealed the presence of an acetoxyl and a tigloyloxyl, which were then attached to the C-13′ and C-15′, respectively, by the HMBC correlations of H_2-13′ and H_2-15′ to their corresponding ester carbonyls (Supplementary data S5). The substantial pyridine-induced solvent shifts (Supplementary data S5) for H_3-14′ ($\Delta\delta$ −0.25) and H-2′β ($\Delta\delta$ −0.26) revealed that they were co-facial with 4′-OH, suggesting that 4′-OH was β-configuration.[15] The relative stereochemistry of **4** was fully verified by the ROESY spectrum (Supplementary data S5).

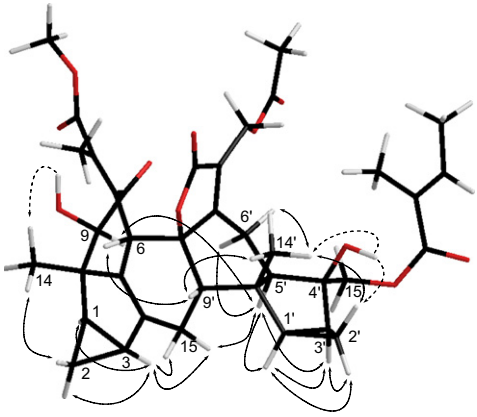

Figure 4. Key ROESY correlations (↔) and important pyridine-induced solvent shifts (⋯→) of chloraholide D (**2**).

2.2. Absolute structures of chlorahololides C–F (1–4)

The exciton chirality method[16] was finally applied to establish the absolute configuration of chlorahololides C–F (**1**–**4**). The UV spectrum of **1** showed a strong absorption at λ_{max} 223 nm (log ε 4.18) corresponding to the moiety of α,β-unsaturated γ-lactone (C-7′, C-11′ and C-12′, Woodward's rules showed ca. 227 nm)[17] and an absorption at λ_{max} 255 nm (log ε 3.81) corresponding to the twisted π-electron system (C-5–C-8 and C-11–C-12). The CD split pattern spectrum (Fig. 5) of **1** matched very well with that reported for two different chromophores at the range of λ_{max} 230–260 nm.[18] The positive Cotton effect at λ_{max} 260 nm ($\Delta\varepsilon$ +26.6) and the negative one at λ_{max} 225 nm ($\Delta\varepsilon$ −24.9) arising from the exciton coupling of a non-degenerate system comprising two different chromophores of the α,β-unsaturated γ-lactone and the twisted π-electron system indicated a positive chirality of **1** (Fig. 5). The absolute configuration of **1** was therefore assigned as depicted.

The CD curves of chlorahololides D–F (**2**–**4**) were very similar in the range of 210–260 nm (Fig. 5), where the first positive Cotton effects (**2**: $\Delta\varepsilon$ +3.90 at λ_{max} 248 nm; **3**: $\Delta\varepsilon$ +3.93 at λ_{max} 252 nm; **4**: $\Delta\varepsilon$ +14.3 at λ_{max} 249 nm) and the second negative Cotton effects (**2**: $\Delta\varepsilon$ −18.1 at λ_{max} 213 nm; **3**: $\Delta\varepsilon$ −25.5 at λ_{max} 225 nm; **4**: $\Delta\varepsilon$ −25.8 at λ_{max} 223 nm) also showed a positive chirality for compounds **2**–**4**. The absolute configuration for compounds **2**–**4** was thus defined as depicted.

2.3. Bioactive evaluation of chlorahololides C–F (1–4)

The activities of chlorahololides C–F (**1**–**4**) on voltage-gated potassium (K^+) channels were examined by using whole

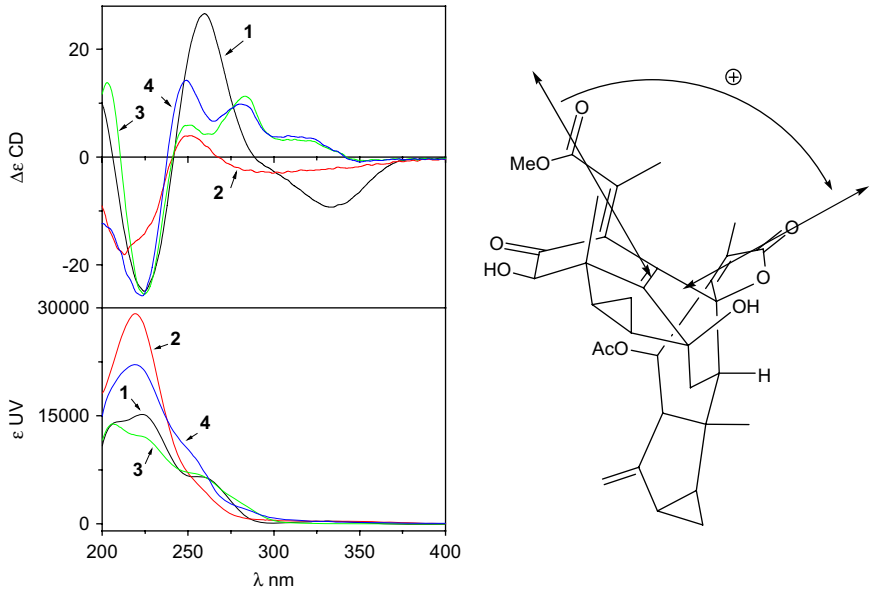

Figure 5. CD and UV spectra of chloraholides C–F (**1**–**4**) measured in MeOH, and the stereoview of **1**, arrows denote the electric transition dipole of the chromophores.

cell voltage-clamp recording in rat dissociated hippocampal neurons, and tetraethylammonium chloride was used as the positive control. Chloraholides C–F (**1**–**4**) exerted potent inhibition on the delayed rectifier K^+ current (I_K) and negligible effect on the fast transient K^+ current (I_A) (Supplementary data S6). The inhibitory IC_{50} values of chloraholides C–F (**1**–**4**) on the delayed rectifier K^+ current (I_K) were 3.6±10.1, 2.7±0.3, 27.5±5.1 and 57.5±6.1 μM, respectively. It is noteworthy that compounds **1**–**4** are 18–388-fold more potent than the positive control tetraethylammonium chloride (IC_{50}: 1.05±0.21 mM), a classical blocker of the delayed rectifier K^+ current.

In conclusion, chloraholides C–F represent a new class of potassium channel blockers, and their potent and selective inhibition on the delayed rectifier (I_K) K^+ current suggests that further investigation into this structural class is warranted. The discovery of these novel sesquiterpenoid dimers, chloraholides C–F, is also a valuable addition to natural products' chemistry, and their interesting structures with significant potassium channel blocking activity also provide an attractive programme for synthetic chemists.

3. Experimental section

3.1. General experimental procedures

Melting points (uncorrected) were determined using a SGW® X-4 apparatus (Shanghai Precision & Scientific Instrument Co., Ltd., China). Optical rotations were measured on a Perkin–Elmer 341 polarimeter (Na filter, λ=589 nm). UV spectra were measured on a Shimadzu UV-2550 spectrophotometer. CD spectrum was measured on a JASCO J-810 instrument. IR spectra were recorded on a Perkin–Elmer 577 spectrometer with KBr disk. ^1H, ^{13}C NMR, ^1H–^1H COSY, HMBC, HSQC, HMQC and ROESY spectra were obtained on Varian Mercury-400, Bruker AM-400 and Varian Inova-600 spectrometers (pyridine-d_5: residual protons at δ_H 8.72, 7.57 and 7.20; $CDCl_3$: TMS as internal standard). EIMS (70 eV) and ESI MS were carried out on a Finnigan MAT 95 mass spectrometer and a Bruker Esquire 3000 plus instruments, respectively. All solvents used were of analytical grade (Shanghai Chemical Plant). Silica gel (200–300 mesh), silica gel H and Sephadex LH-20 were used for column chromatography, and percolated silica gel GF_{254} plates (Qingdao Haiyang Chemical Plant, Qingdao, People's Republic of China) were used for TLC. C18 reversed-phase silica gel (250 mesh, Merck) and MCI gel (CHP20P, 75–150 μm, Mitsubishi Chemical Industries Ltd.) were also used for column chromatography.

3.2. Plant material

The plant material of *C. holostegius* was collected from Xishuangbanna Tropical Botanical Garden (XTBG), Mengla County, Yunnan province of China in July 2005, and was authenticated by Prof. You-Kai Xu of Xishuangbanna Tropical Botanical Garden, Chinese Academy of Sciences. A voucher specimen has been deposited at Shanghai Institute of *Materia Medica* (Accession number: CH-2005-2Y).

3.3. Extraction and isolation

The air-dried powder (1.0 kg) of stems and leaves of *C. holostegius* was percolated three times with 95% EtOH to give the crude extract (140 g). This was partitioned between EtOAc and water to afford EtOAc-soluble portion (130 g), which was subsequently subjected to a MCI gel column chromatography eluted with aqueous CH_3OH in gradient (50–100%, v/v) to obtain seven major fractions 1–7 (as monitored by TLC). Fractions 4–6 contained mainly sesquiterpenoid

dimers. Fraction 4 (3.30 g) was chromatographed over a silica gel column ($CHCl_3$/MeOH, 75:1) to give two major components F4a and F4b. F4a was purified by using a reversed-phase C-18 silica gel column (aqueous CH_3OH, 70%) to give chloraahololide B (0.001%).[9d] F4b was purified by a reversed-phase C-18 silica gel column (aqueous CH_3OH, 70%), followed by a Sephadex LH-20 column (CH_3OH) to yield **3** (0.03 g, 0.003%). Fraction 5 (6.56 g) was separated into two major subfractions F5a and F5b on a silica gel column ($CHCl_3$/MeOH, 100:0–50:1), and each of them (F5a and F5b) was purified, respectively, by a similar procedure of a reversed-phase C-18 silica gel column (aqueous CH_3OH, 60%), and then a Sephadex LH-20 (CH_3OH) to afford **1** (0.23 g, 0.023%) and **4** (0.01 g, 0.001%). By the same procedure as applied in the treatment of fraction 5, fraction 6 (3.24 g) afforded chloraahololide A (0.008%)[9d] and compound **2** (0.02 g, 0.002%).

3.4. Chloraahololide C (*1*)

Tiny prismatic solid; mp: 145–147 °C; $[\alpha]_D^{20}$ −143 (*c* 0.212, MeOH); UV (MeOH, log *ε*) λ_{max} 255 (3.81), 223 (4.18) nm; CD (MeOH, Δ*ε*) λ_{max} 334 (−9.28), 260 (+26.6), 225 (−24.9) nm; IR (KBr, disc) λ_{max} 3479, 2943, 1755, 1709, 1608, 1437, 1379, 1294, 1225, 1115, 968 cm^{-1}; for ^{13}C NMR data see Table 1 and ^1H NMR see Table 2; EIMS 70 eV *m/z* (rel int) 576 $[M]^+$ (6), 558 (20), 544 (10), 516 (100), 487 (34), 456 (55), 443 (57), 411 (83), 383 (66), 365 (75), 351 (61), 323 (64), 295 (46), 272 (37), 243 (55), 227 (82), 213 (94), 183 (41), 157 (66), 119 (63), 105 (98), 91 (85), 55 (29); ESI MS (positive) *m/z* 599 $[M+Na]^+$; HREIMS (*m/z*) calcd for $C_{33}H_{36}O_9$, 576.2359; found, 576.2359 $[M]^+$.

3.5. Chloraahololide D (*2*)

White powder; mp: 170–172 °C; $[\alpha]_D^{20}$ −121 (*c* 0.225, MeOH); UV (MeOH, log *ε*) λ_{max} 220 (4.65) nm; CD (MeOH, Δ*ε*) λ_{max} 248 (+3.90), 213 (−18.1) nm; IR (KBr, disc) λ_{max} 3467, 2985, 1763, 1736, 1691, 1645, 1439, 1259, 1234, 1084, 987, 739 cm^{-1}; for ^{13}C NMR data see Table 1 and ^1H NMR see Table 2; EIMS 70 eV *m/z* (rel int) 676 $[M]^+$ (0.07), 616 (0.4), 556 (0.6), 513 (0.7), 402 (5), 274 (14), 242 (7), 224 (100), 209 (35), 196 (25), 157 (12), 141 (9), 91 (5), 83 (70), 55 (28); ESI MS (positive) *m/z* 699 $[M+Na]^+$; HREIMS (*m/z*) calcd for $C_{38}H_{44}O_{11}$, 676.2884; found, 676.2850 $[M]^+$.

3.6. Chloraahololide E (*3*)

White powder; mp: 157–159 °C; $[\alpha]_D^{20}$ +97 (*c* 0.0975, MeOH); UV (MeOH, log *ε*) λ_{max} 206 (4.14) nm; CD (MeOH, Δ*ε*) λ_{max} 283 (+11.3), 264 (+4.23), 252 (+5.93), 225 (−25.5), 203 (+13.8) nm; IR (KBr, disc) λ_{max} 3439, 2929, 1770, 1743, 1371, 1229, 1111, 1020, 970, 742 cm^{-1}; for ^{13}C NMR data see Table 1 and ^1H NMR see Table 2; EIMS 70 eV *m/z* (rel int) 560 $[M]^+$ (0.06), 542 (0.07), 500 (2), 472 (16), 439 (11), 411 (13), 393 (10), 365 (13), 351 (90), 333 (23), 305 (37), 279 (20), 226 (41), 184 (28), 157 (25), 121 (100), 91 (41), 77 (18), 55 (15); ESI MS (positive) *m/z* 1143.5 $[2M+Na]^+$, 583 $[M+Na]^+$; HREIMS (*m/z*) calcd for $C_{32}H_{32}O_9$, 560.2046; found, 560.2071 $[M]^+$.

3.7. Chloraahololide F (*4*)

White powder; mp: 141–143 °C; $[\alpha]_D^{20}$ +30 (*c* 0.147, MeOH); UV (MeOH, log *ε*) λ_{max} 219 (4.34) nm; CD (MeOH, Δ*ε*) λ_{max} 280 (+9.84), 265 (+6.63), 249 (+14.3), 223 (−25.8) nm; IR (KBr, disc) λ_{max} 3454, 2933, 1755, 1651, 1441, 1381, 1263, 1229, 1146, 1028, 970 cm^{-1}; for ^{13}C NMR data see Table 1 and ^1H NMR see Table 2; EIMS 70 eV *m/z* (rel int) 676 $[M]^+$ (0.2), 642 (0.2), 606 (1.3), 578 (1), 500 (2), 470 (5), 427 (5), 395 (6), 381 (7), 351 (8), 323 (7), 289 (10), 257 (9), 239 (11), 215 (11), 155 (11), 128 (12), 105 (16), 91 (16), 83 (100), 60 (92); ESI MS (negative) *m/z* 1351.5 $[2M-H]^-$; HREIMS (*m/z*) calcd for $C_{37}H_{40}O_{12}$, 676.2520; found, 676.2508 $[M]^+$.

3.8. Electrophysiological assay of chloraahololides C–F (*1–4*) on potassium (K^+) channels

The effects of chloraahololides C–F (**1–4**) on voltage-gated potassium (K^+) channels were investigated according to the standard protocols reported in the literature,[4] and tetraethylammonium chloride, a classical blocker of the delayed rectifier K^+ current, as the positive control.

Acknowledgements

Financial support of the National Natural Science Foundation (Grant No. 30630072; 20702057) of PR China is gratefully acknowledged. We thank Prof. You-Kai Xu of Xishuangbanna Tropical Botanical Garden, Chinese Academy of Sciences for the collection and identification of the plant material. We also thank Prof. W. Kitching, Department of Chemistry, the University of Queensland, Australia, for reading this manuscript.

Supplementary data

Supplementary data associated with this article can be found in the online version, at doi:10.1016/j.tet.2007.12.057.

References and notes

1. Shieh, C. C.; Coghlan, M.; Sullivan, J. P.; Gopalakrishnan, M. *Pharmacol. Rev.* **2000**, *52*, 557–593.
2. (a) Yu, S. P.; Yeh, C. H.; Sensi, S. L.; Gwag, B. J.; Canzoniero, L. M. T.; Farhangrazi, Z. S.; Ying, H. S.; Tian, M.; Dugan, L. L.; Choi, D. W. *Science* **1997**, *278*, 114–117; (b) Yu, S. P.; Yeh, C. H.; Gottron, F.; Wang, X.; Grabb, M. C.; Choi, D. W. *J. Neurochem.* **1999**, *73*, 933–941.
3. (a) Jiao, S.; Wu, M. M.; Hu, C. L.; Zhang, Z. H.; Mei, Y. A. *J. Pineal. Res.* **2004**, *36*, 109–116; (b) Hu, C. L.; Liu, Z.; Gao, Z. Y.; Zhang, Z. H.; Mei, Y. A. *J. Pineal. Res.* **2005**, *38*, 53–61.
4. Liu, H.; Li, Y.; Song, M. K.; Tan, X. J.; Cheng, F.; Zheng, S. X.; Sheng, J. H.; Luo, X. M.; Ji, L. Y.; Yue, J. M.; Hu, G. Y.; Jiang, H. L.; Chen, K. X. *Chem. Biol.* **2003**, *10*, 1103–1113.
5. Zhou, Z. K. *Yunnan Zhiwu Yanjiu* **1993**, *15*, 321–331.
6. Chen, Y. Q.; Cheng, D. Z.; Wu, G. F.; Cheng, P. S.; Zhu, P. Z. *Chinese Flora (Zhongguo Zhiwu Zhi)*; Science: Beijing, 1982; Vol. 20, pp 80–96.

7. Editorial Committee (over 300 members) of the Administration Bureau of Traditional Chinese Medicine. *Chinese Materia Medica (Zhonghua Benchao)*; Shanghai Science and Technology: Shanghai, 1998; Vol. 3, pp 451–452.
8. (a) Kawabata, J.; Mizutani, J. *Agric. Biol. Chem.* **1989**, *53*, 203–207; (b) Kawabata, J.; Mizutani, J. *Agric. Biol. Chem.* **1988**, *52*, 2965–2966; (c) Kawabata, J.; Fukushi, Y.; Tahara, S.; Mizutani, J. *Agric. Biol. Chem.* **1985**, *49*, 1479–1485.
9. (a) Kawabata, J.; Fukushi, E.; Mizutani, J. *Phytochemistry* **1998**, *47*, 231–235; (b) Kawabata, J.; Fukushi, E.; Mizutani, J. *Phytochemistry* **1995**, *39*, 121–125; (c) Yang, S. P.; Yue, J. M. *Tetrahedron Lett.* **2006**, *47*, 1129–1132; (d) Yang, S. P.; Gao, Z. B.; Wang, F. D.; Liao, S. G.; Chen, H. D.; Zhang, C. R.; Hu, G. Y.; Yue, J. M. *Org. Lett.* **2007**, *9*, 903–906.
10. Kwon, O. E.; Lee, H. S.; Lee, S. W.; Bae, K.; Kim, K.; Hayashi, M.; Rho, M. C.; Kim, Y. K. *J. Ethnopharmacol.* **2006**, *104*, 270–277.
11. Gao, C. W.; Chen, Y. S.; Xie, J. M.; Zhao, S. N. *Gaodeng Xuexiao Huaxue Xuebao* **1987**, *8*, 141–142.
12. Oikawa, H.; Suzuki, Y.; Naya, A.; Katayama, K.; Ichihara, A. *J. Am. Chem. Soc.* **1994**, *116*, 3605–3606.
13. Oppolzer, W. *Comprehensive Organic Synthesis*; Trost, B. M., Fleming, I., Eds.; Pergamon: Oxford, 1991; Vol. 5, pp 315–399.
14. (a) Yang, S. P.; Cheng, J. G.; Huo, J.; Jiang, H. L.; Chen, K. X.; Yue, J. M. *Chin. J. Chem.* **2005**, *23*, 1530–1536; (b) Yang, S. P.; Huo, J.; Wang, Y.; Lou, L. G.; Yue, J. M. *J. Nat. Prod.* **2004**, *67*, 638–643.
15. Demacro, P. V.; Farkas, E.; Doddrell, D.; Mylari, B. L.; Wenkert, E. *J. Am. Chem. Soc.* **1968**, *90*, 5480–5486.
16. Harada, N.; Nakanishi, K.; Tatsuoka, S. *J. Am. Chem. Soc.* **1969**, *91*, 5896–5898.
17. Pretsch, E.; Bühlmann, P.; Affolter, C. *Structure Determination of Organic Compounds: Tables of spectral Data;* Chinese Version, Translated by Rong, G. B.; Zhu, S. Z.; East China University of Science and Technology: Shanghai, 2002; pp 388–389.
18. Harada, N.; Nakanishi, K. *Circular Dichroic Spectroscopy: Exciton Coupling in Organic Stereochemistry*, 1st ed.; Oxford University Press: Oxford, 1983; pp 85–87.